Pak. J. Bot., 52(3), 735-752, 2020. DOI: http://dx.doi.org/10.30848/PJB2020-3(8)

SALT STRESS RESISTANCE IN *SMCP*-TRANSGENIC *ARABIDOPSIS THALIANA* AS REVEALED BY TRANSCRIPTOME ANALYSIS

HE Lİ[1,2,3#], LİU ZHENG[1,2#], YİNG WANG[1,2], XİANQİ HU[3], ZHUCHOU LU[1,2], HUİJİN FAN[1,2], ZHUANG ZHANG[1,2], YİXİAO Lİ[4], RENYİNG ZHUO[1,2*], WENMİN QİU[1,2*]

[1]*State Key Laboratory of Tree Genetics and Breeding, Chinese Academy of Forestry, Xiangshan Road, Beijing, 100091, China*
[2]*The Research Institute of Subtropical Forestry, Chinese Academy of Forestry, Fuyang, Hangzhou, Zhejiang, 311400, China*
[3]*College of Plant Protection, Yunnan Agricultural University, Kunming 650201, China*
[4]*Productivity promotion center of Hangzhou, Hangzhou 310012, China*
[#]*These authors contributed equally to this work*
[*]*Corresponding author's email: qiuwm05@163.com; zhuory@gmail.com; TEL: 0571-63311860*

Abstract

Adaptation to environmental changes is crucial for the viability of all organisms. In plants, cysteine proteases (CP) are vital proteolytic enzymes response to complex and volatile environmental factors. Previously, over-expression of a CP gene isolated from *Salix matsudana* (*SmCP*) was shown to improve the salt stress tolerance of *Arabidopsis thaliana*. However, the molecular mechanisms that underlie the enhanced salt stress tolerance of these over-expression lines remain uncharacterized. In this study, the transcriptome of transgenic *Arabidopsis SmCP* over-expression lines and wild type (WT) control (CT) plants was analyzed by RNA sequencing to identify genes associated with salt tolerance. The abundance level of selected differentially expressed genes was validated by quantitative real-time PCR analysis. The *SmCP*-transgenic line showed many transcriptomic changes under salt-stress conditions, including genes associated with alterations in the anti-oxidant environment and ion-transport capacity. Elucidation of the mechanism of salt stress resistance is important for utilization of *SmCP* for genetic improvement of commercial crops for tolerance to saline soil.

Key words: *SmCP*, Salt stress, Transcriptome.

Introduction

Soil salinity is a serious environmental factor that limits seed germination and plant growth (Yang & Guo, 2018; Rahat *et al.*, 2019). After exposure for several minutes to salt stress (SS), rapid changes in osmotic potential internal and external to the plant occur, resulting in water deficit and wilting of plants (Munns, 2002; Fricke *et al.*, 2006; Alzahrani *et al.*, 2019). A global area of 800 million ha is affected by salt, and this problem is continuously deteriorating the situation (Munns & Tester, 2008). Plants have specific mechanisms to reduce and alleviate the effects of salt. Based on the tolerance of plants to salt stress, plants can be classified as either salt-intolerant glycophytes, such as citrus and tomato, or salt-resistant halophytes, such as cotton and barley (Park *et al.*, 2016).

Salix matsudana is a salt-resistant tree species that is potentially suitable for the screening of salt tolerance genes. A salt tolerance-related cysteine protease (CP) gene was previously isolated from a salt stress-induced cDNA library from *S. matsudana* and contains the typical Cys-His-Asn triad of the active site (Zheng *et al.*, 2018). Cysteine protease genes perform crucial functions in the programmed cell death (PCD) pathway of animals (Stanczykiewicz *et al.*, 2017). The induction of CP in plant systems undergoing PCD has been demonstrated (Minami & Fukuda, 1995; Ye & Varner, 1996). Cell death involving PCD is broadly separated into developmentally regulated and environmentally induced processes. Cysteine proteases are important in aging (van Wyk *et al.*, 2014) and play a key role in proteolysis of higher plants from embryonic development to certain forms of cell aging (Tajima *et al.*, 2011). The involvement of CP in nodule senescence has also been reported (Lee *et al.*, 2004; van Wyk *et al.*, 2014). Under environmental stress, CP participates in diverse physiological processes, such as plant anabolism and catabolism, withering and abscission, tissue senescence, and seed development (Ao *et al.*, 2016). Cysteine proteases are considered to be an important component of the regulation of oxidative protein degradation and reactive oxygen species (ROS) concentrations (van der Hoorn, 2008). The CP gene *RD21* was a salt stress-responsive gene induced by water deficiency(Koizumi *et al.*, 1993; Hayashi *et al.*, 2001). Over-expression of *SmCP* in *A. thaliana* increased resistance to salt stress (Zheng *et al.*, 2018). Genetic modulation of the activity of endogenous CP may be important for the future engineering of plant salt stress tolerance. Genome and transcriptome sequencing using next generation sequencing technology are commonly used for candidate genes mining (Sun *et al.*, 2013). High-throughput sequencing show**ed** great advantages in quantitative large scale of gene expression (Liu *et al.*, 2016).

In this study, we used Illumina paired-end sequencing technology to analyze the transcriptomes of two genotypes of *A. thaliana* (*SmCP* over-expression and un-transformed lines) exposed to salt-stress and non-salt-stress treatments. The objective was to dissect the molecular mechanisms underlying the contrasting morpho-physiological traits of the two genotypes. We hypothesized that co-ordination of a balanced anti-oxidant environment and ion transport may be important for the enhanced salt-stress tolerance in *SmCP* over-expression lines of *A. thaliana*.

Materials and Methods

Plant materials and salt-stress treatment: In this experiment, the *SmCP* gene was overexpressed in *A. thaliana* under the control of the CaMV 35S promoter. Wild type (WT; *A. thaliana* ecotype Columbia) and *SmCP*-transgenic plants were grown in organic soil for 1 month, then for 12 plants of each genotype the soil was irrigated with 100 mM NaCl as salt-stress treatment. As the untreated control, the same number of WT and transgenic plants were irrigated with water at the same time. After salt stress treatment for 1 week, fresh leaves of WT and transgenic plants from the salt-stress treatment and untreated control were gathered, immediately frozen in liquid nitrogen, and stored until extraction of total RNAs. Three independent biological replicates were sampled for RNA sequencing (RNA-seq) and qRT-PCR analysis.

cDNA library construction and RNA sequencing: Total RNAs were extracted using the RNAsimple Total RNA Kit (TIANGEN, Beijing, China) in accordance with the manufacturer's instructions. Magnetic beads conjugated with oligo (dT) were used for preparation of enriched mRNAs, which served as the template for cDNA library construction. Twelve cDNA libraries were constructed and then sequenced using an Illumina HiSeq platform by BMK (Beijing, China).

Gene expression and differential gene expression analysis: The raw reads were cleaned by deleting the reads containing adaptor sequences and low-quality reads (the proportion of N was greater than 10%; the base number of the quality score Q<10 accounted for more than 50% of the entire read). The *A. thaliana* TAIR10 genome (https://www.arabidopsis.org/index.jsp) was used as the reference genome. Clean reads were mapped to the reference genome using TopHat2 (Kim *et al.*, 2013). Cufflinks was used to calculate the fragments per kilobase of transcript sequence per million mapped reads (FPKM) as an estimate of gene expression to normalize the number of mapped reads and transcript length (Mortazavi *et al.*, 2008; Trapnell *et al.*, 2013; Xu *et al.*, 2013). DEGs were screened using the DESeq package; a unigene with an adjusted *P*-value <0.05 and fold change > 2 was considered to show significant differences in expression. Functional analysis of DEGs was carried out using the DAVID 6.7 tool (http://david.ncifcrf.gov/) (Huang da *et al.*, 2009a, 2009b).

Functional annotation and enrichment of DEGs: The unigene sequences of DEGs were aligned to the Gene Ontology Consortium (GO), Kyoto Encyclopedia of Genes and Genomes (KEGG), and Cluster of Orthologous Groups of proteins (COG) databases for gene annotation and functional classification. Functional enrichment analysis was performed using the AmiGO and KOBAS online tools. The selected genes were subjected to cluster analysis using the CLUSTER program.

Quantitative real-time PCR analysis: To evaluate the credibility of the RNA-seq results, the data were validated using quantitative real-time PCR (qRT-PCR) analysis. Nine up-regulated and seven down-regulated DEGs were selected for validation. Total RNA extraction was consistent with the afore-mentioned method. First-strand cDNA synthesis and the qRT-PCR procedure followed the methods of Han (Han *et al.*, 2016). Three biological replicates were performed for each sample, and the relative expression level was calculated using ratio = $2^{-\Delta\Delta Ct}$. The names of the genes used for qRT-PCR analysis and the primer sequences used are listed in Table 1.

Results

RNA-seq and reference-guided assembly: In total, 182.61 Gb clean RNA-seq data was obtained from 12 tissue samples (on average 12.64 Gb clean data for each sample). The percentage of bases with a quality score of 30 (Q30) was at least 88.6%. Overall, about 90% (ranging from 89.75% to 91.82% for individual samples) of clean reads were mapped to the *Arabidopsis* TAIR10 reference genome. A summary of the Illumina transcriptome sequence data was presented in the Table S1a and the alignment efficiency was summarized in the Table S1b.

Effects of the *SmCP* transgene on the transcriptome under salt stress: A total of 2,570 genes were identified as DEGs (differentially expressed genes) (Fig. 1), consisting of 1,742 genes that were up-regulated and 828 genes that were down-regulated, by comparison of gene expression levels of *SmCP*-transgenic and WT plants without salt stress. Thirty-two genes were differentially-expressed between WT and *SmCP*-transgenic plants under salt stress, of which 16 genes were up-regulated and 16 genes were down-regulated. To characterize patterns of differential gene expression in plants of each genotype in response to salt stress, a heatmap cluster of the expression pattern of DEGs under salt-stress and non-salt-stress conditions was constructed (Fig. 2). The DEGs showed different magnitudes of up- and down-regulation for different groups of genes response to salt stress.

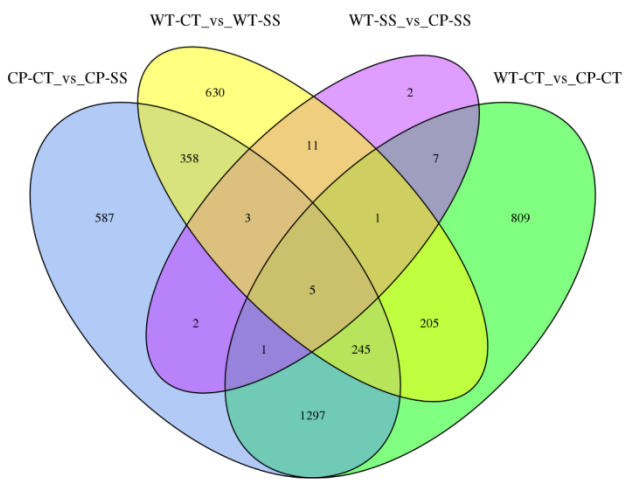

Fig. 1. **Venn diagram of genes differentially expressed in four comparisons.** The diagram was drawn according to the functional annotation of unigenes and the specific clustering analysis data. CP-CT, *SmCP*-transgenic lines control; CP-SS, *SmCP*-transgenic lines under salt stress; WT-CT, wild-type control; WT-SS, wild type under salt stress.

Table 1. Primers used in the study.

Application	Name	Sequence(5' - 3')
SmCP qRT-PCR primers	*SmCP*-RT-F	GGGCTTGCCTTACACTCTTGGTC
	SmCP-RT-R	GCCTTCTTCCCTCCAGTCTTTCG
A. thaliana reference gene ACTIN primers	Actin-F	GCACCCTGTTCTTCTTACCG
	Actin-R	AACCCTCGTAGATTGGCACA
A. thaliana transcriptome qRT - PCR primers	AT1G56650-F	CGACTGCAACCATCTCAATG
	AT1G56650-R	AGGTGTCCCCCTTTTCTGTT
	AT1G60000-F	CCGCCGTTAACACTAAGCTC
	AT1G60000-R	GCAATCTTCGACATTGCTCA
	AT5G26340-F	CAGGCAGGATATTGCTTGG
	AT5G26340-R	TTTACTTGGCGGTCCCATAG
	AT5G44190-F	TACTAGCGCGTGAAGCAGA
	AT5G44190-R	ATTGGATACGTCCGATGAGC
	AT1G55450-F	TCTAATCGTGGCAGCACAA
	AT1G55450-R	TTCTAAACGGGAACGTGGAG
	AT1G54820-F	AATGCCCATATTTGGTGGA
	AT1G54820-R	CACTTGAAGTTCCGGTGGAT
	AT4G35770-F	AATGAGCTGCCGGTAGAAG
	AT4G35770-R	ATCCCCGTCCTTAATTGGTC
	AT4G21990-F	GCTGCGGGTTATGTTTCAAT
	AT4G21990-R	TGCCTGCTCAAGTTCACAAC
	AT3G21250-F	AGAGCGGTTATGTTGGGAT
	AT3G21250-R	CCAAGATGGGCAGTCGTAAT
	AT4G02520-F	CTCAAAGACGGTGAGCAC
	AT4G02520-R	TGATGCATGGAAAAGGTTCA
	AT2G29450-F	TGAAGCTTTTGGGGATATG
	AT2G29450-R	GGATTTTGTGGCCAAGTCTC
	AT4G16190-F	AAACCAAGAAGCATGGATC
	AT4G16190-R	CTGCGTTGAGGAGTTGTTCA
	AT5G62350-F	CGTCTCGCGTCTAACACGT
	AT5G62350-R	ATCGGAGCAAGTGTTCTCGT
	AT3G03920-F	GATGCTTTTGACGGGTTTG
	AT3G03920-R	CGGAGCGTTAAAATGAGGAA
	AT5G26340-F	FCAGGCAGGATATTGCTTGGT
	AT5G26340-R	TTTACTTGGCGGTCCCATAG

Table S1a. Summary of Illumina transcriptome sequencing results.

Samples	Clean reads	Clean bases	GC Content	% ≥ Q30
WT-CT1	52613919	15692100030	0.4679	0.913
WT-CT2	50760811	15139567152	0.4646	0.8886
WT-CT3	53495586	16081473848	0.4659	0.9074
CP-CT1	42350790	12644621988	0.4644	0.9089
CP-CT2	44925284	13424788810	0.4637	0.9094
CP-CT3	46694287	13985490274	0.4619	0.9102
WT-SS1	49065456	14676804356	0.4599	0.9083
WT-SS2	54254460	16242859070	0.4637	0.9067
WT-SS3	50786191	15186172678	0.4607	0.9113
CP-SS1	59996544	17955618986	0.4636	0.9088
CP-SS2	50901184	15238257290	0.461	0.9103
CP-SS3	54937968	16344167338	0.4657	0.9166

Table S1b. Summary of Illumina transcriptome sequencing alignment efficiency.

Samples	Total reads	Mapped reads	Uniq mapped reads	Multiple reads	Reads map to'+'	Reads map to'-'
WT - CT1	105227838	96,623,241 (91.82 %)	94,956,731 (90.24 %)	1,666,510 (1.58 %)	47,975,548 (45.59 %)	47,973,406 (45.59 %)
WT - CT2	101521622	91,700,354 (90.33 %)	89,763,265 (88.42 %)	1,937,089 (1.91 %)	45,466,934 (44.79 %)	45,459,263 (44.78 %)
WT - CT3	106991172	97,754,951 (91.37 %)	96,188,003 (89.90 %)	1,566,948 (1.46 %)	48,632,904 (45.46 %)	48,629,700 (45.45 %)
CP - CT1	84701580	76,018,254 (89.75 %)	74,247,674 (87.66 %)	1,770,580 (2.09 %)	37,656,382 (44.46 %)	37,647,447 (44.45 %)
CP - CT2	89850568	81,170,346 (90.34 %)	79,440,455 (88.41 %)	1,729,891 (1.93 %)	40,279,690 (44.83 %)	40,271,362 (44.82 %)
CP - CT3	93388574	84,674,611 (90.67 %)	83,054,909 (88.93 %)	1,619,702 (1.73 %)	42,079,578 (45.06 %)	42,057,315 (45.03 %)
WT - SS1	98130912	88,694,132 (90.38 %)	87,377,980 (89.04 %)	1,316,152 (1.34 %)	44,159,372 (45.00 %)	44,153,583 (44.99 %)
WT - SS2	108508920	98,517,319 (90.79 %)	95,397,414 (87.92 %)	3,119,905 (2.88 %)	48,676,921 (44.86 %)	48,675,718 (44.86 %)
WT - SS3	101572382	92,190,673 (90.76 %)	89,615,588 (88.23 %)	2,575,085 (2.54 %)	45,634,375 (44.93 %)	45,635,228 (44.93 %)
CP - SS1	119993088	108,541,380 (90.46 %)	105,323,740 (87.77 %)	3,217,640 (2.68 %)	53,631,782 (44.70 %)	53,646,614 (44.71 %)
CP - SS2	101802368	92,114,629 (90.48 %)	90,582,887 (88.98 %)	1,531,742 (1.50 %)	45,833,823 (45.02 %)	45,850,571 (45.04 %)
CP - SS3	109875936	99,289,302 (90.36 %)	96,763,776 (88.07 %)	2,525,526 (2.30 %)	49,246,900 (44.82 %)	49,251,167 (44.82 %)

The DEGs were subjected to functional annotation and gene ontology (GO) enrichment analysis. In *SmCP*-transgenic plants, the most highly enriched GO terms for the salt-induced DEGs were 'structural constituent of ribosome' (GO: 0003735), 'DNA replication initiation' (GO: 0006270), and 'cell proliferation process' (GO: 0008283) in the Biological Processes category. Compared with the WT, enriched GO terms for DEGs were predominantly associated with biological processes, for example 'zinc ion response' (GO: 0010043), 'response to growth hormone' (GO: 0060416), and 'sequestering of metal ion' (GO: 0051238) were enriched in *SmCP*-transgenic plants under salt-stress treatment (Fig. 3, Table S2).

By comparison of DEGs for the two genotypes under the salt-stress and non-stress treatments, we obtained a significant enrichment pathway for up-regulation and down-regulation of DEGs. Salt-stress showed different effects on both WT and *SmCP*-transgenic DEGs (Figs. 4 and 5). The most significantly enriched pathways in *SmCP*-transgenic plants under salt stress were 'ribosome', 'DNA replication', 'cutin, suberin, and wax biosynthesis', and 'Circadian rhythm - plant' (Table S3). However, the most highly enriched pathways of WT DEGs under salt stress were involved in 'plant hormone signal transduction', 'photosynthesis-antenna proteins', 'DNA replication', 'phenylpropanoid biosynthesis', and 'pentose and glucuronate inter-conversions'. In addition, the salt-stress-associated pathway 'glutathione metabolism' (ko00480) was highly enriched among DEGs in CP-SS vs WT-SS (*SmCP*-transgenic under salt stress vs wildtype under salt stress) comparisons.

DEGs involved in salt stress associated with *SmCP* transgenic: With regard to the CP-SS vs WT-SS comparison, many DEGs were annotated with GO terms involved in cation binding and transport, which contributed to the genotypic differences in salt tolerance, such as 'metal ion binding' (GO: 0046872), 'chlorophyll catabolite transmembrane transporter activity' (GO: 0010290), 'cation binding' (GO: 0043169), and 'transporter activity' (GO:0005215). Metal transporters and cation channels belonging to different protein families, such as an ABC transporter (*AT3G59140*) and a member of the NRT1/PTR family (*AT1G22550*), showed differential expression in the CP-SS vs WT-SS comparison. Redox-associated GO terms, such as 'glutathione peroxidase activity' (GO: 0004602) and 'protein disulfide oxidoreductase activity' (GO: 0015035), also showed significant changes in expression pattern. These results indicated that the mechanisms of salt tolerance of *SmCP*-transgenic *A. thaliana* involved membrane transporter-related and anti-oxidant related proteins.

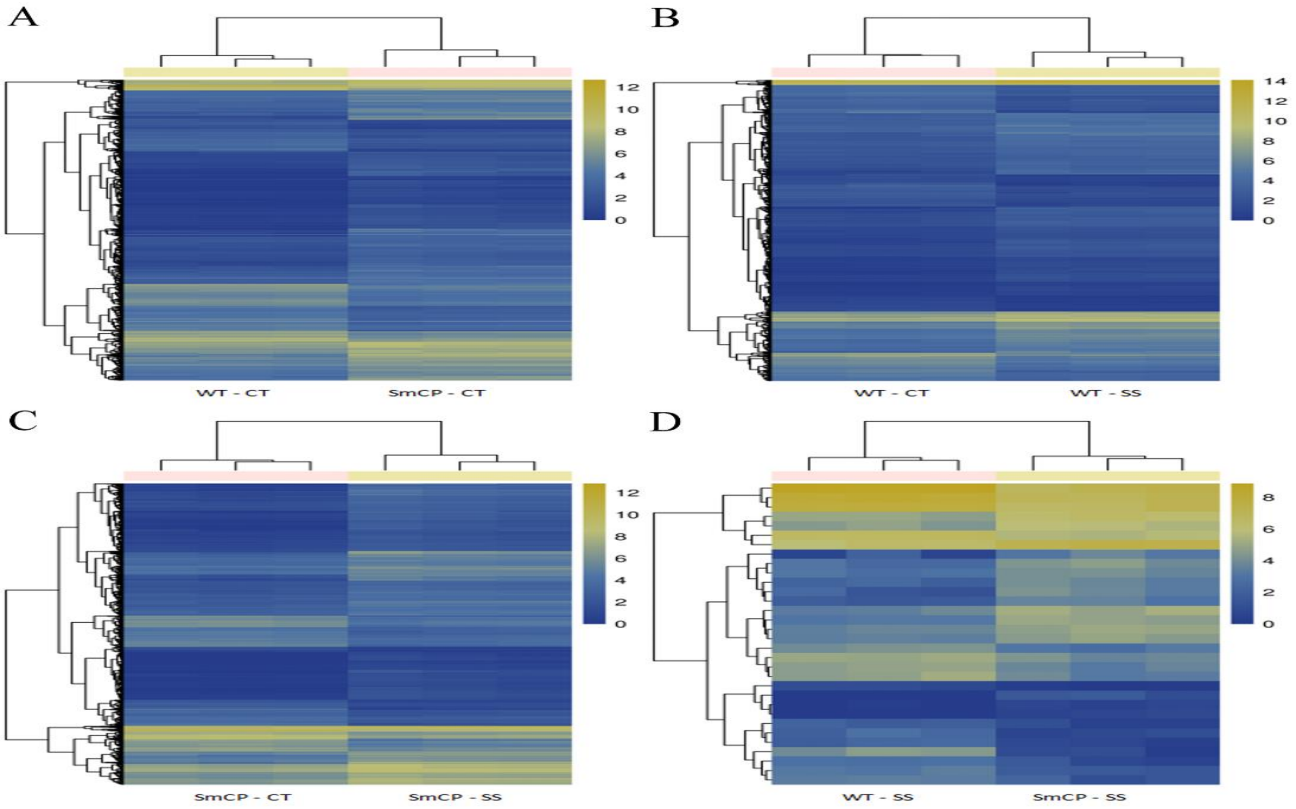

Fig. 2. **Cluster analysis of differentially expressed genes.** (A) Wild-type control and *SmCP*-transgenic control comparison. (B) Wild-type control and wild type under salt stress comparison. (C) *SmCP*-transgenic control and *SmCP*-transgenic under salt stress comparison. (D) Wild-type and *SmCP*-transgenic under salt stress comparison. CP-CT, *SmCP*-transgenic lines control; CP-SS, *SmCP*-transgenic lines under salt stress; WT-CT, wild-type control; WT-SS, wild type under salt stress.

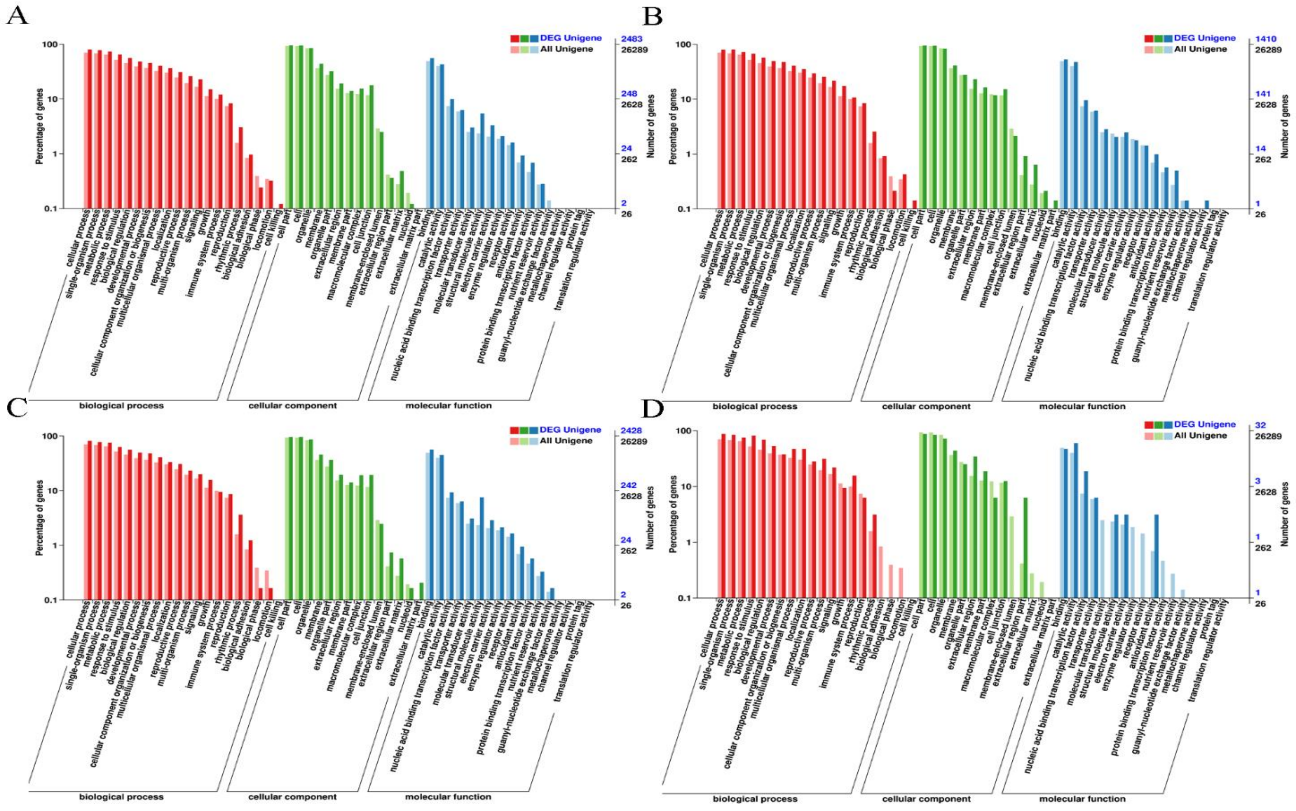

Fig. 3. **Functional annotation and gene ontology analysis.** (A) Wild-type control and *SmCP*-transgenic lines control comparison. (B) Wild-type control and wild type under salt stress comparison. (C) *SmCP*-transgenic lines control and *SmCP*-transgenic lines under salt stress comparison. (D) Wild type under salt stress and *SmCP*-transgenic lines under salt stress comparison.

Table S2. Enrichment of GO terms among differentially expressed genes from four comparisons of *SmCP*-transgenic lines and the wild type determined using the top GO software package.

GO.ID	Term	*Q* - value
	WT-CT VS CP-CT	
GO:0001510	RNA methylation	2.00E-20
GO:0006275	regulation of DNA replication	6.10E-14
GO:0006270	DNA replication initiation	1.20E-12
GO:0009611	response to wounding	1.30E-12
GO:0008283	cell proliferation	4.30E-12
GO:0010389	regulation of G2/M transition of mitotic cell cycle	1.70E-10
GO:0051567	histone H3-K9 methylation	3.40E-10
GO:0000911	cytokinesis by cell plate formation	4.80E-09
GO:0048453	sepal formation	2.30E-08
GO:0048451	petal formation	3.70E-08
GO:0009612	response to mechanical stimulus	8.00E-08
GO:0080167	response to karrikin	6.70E-07
GO:0051225	spindle assembly	1.20E-06
GO:0051238	sequestering of metal ion	1.50E-06
GO:0007018	microtubule-based movement	2.00E-06
GO:0010200	response to chitin	2.70E-06
GO:0000966	RNA 5'-end processing	3.60E-06
GO:0009409	response to cold	5.70E-06
GO:0006306	DNA methylation	7.40E-06
GO:0016572	histone phosphorylation	8.40E-06
GO:0080175	phragmoplast microtubule organization	1.50E-05
GO:0033506	glucosinolate biosynthetic process from homomethionine	1.50E-05
GO:0009686	gibberellin biosynthetic process	1.90E-05
GO:0032508	DNA duplex unwinding	2.60E-05
GO:0050832	defense response to fungus	3.70E-05
GO:0010167	response to nitrate	3.70E-05
GO:0019605	butyrate metabolic process	3.90E-05
GO:0015706	nitrate transport	5.10E-05
GO:0009753	response to jasmonic acid	7.70E-05
GO:0009414	response to water deprivation	7.70E-05
GO:0002679	respiratory burst involved in defense response	9.00E-05
GO:0022625	cytosolic large ribosomal subunit	2.50E-11
GO:0005730	nucleolus	5.20E-11
GO:0009506	plasmodesma	1.50E-09
GO:0009505	plant-type cell wall	4.20E-09
GO:0005871	kinesin complex	1.70E-07
GO:0022627	cytosolic small ribosomal subunit	1.80E-07
GO:0005886	plasma membrane	3.00E-07
GO:0005794	Golgi apparatus	1.70E-06
GO:0005874	microtubule	9.30E-06
GO:0048046	apoplast	2.30E-05
GO:0005618	cell wall	3.90E-05
GO:0097014	ciliary cytoplasm	6.70E-05
GO:0003735	structural constituent of ribosome	8.00E-10
GO:0043295	glutathione binding	1.80E-06
GO:0004016	adenylate cyclase activity	2.00E-06
GO:0008574	plus-end-directed microtubule motor activity	2.80E-06
GO:0016762	xyloglucan:xyloglucosyl transferase activity	5.40E-06
GO:0004364	glutathione transferase activity	5.90E-06
GO:0080039	xyloglucan endotransglucosylase activity	1.20E-05
GO:0080102	3-methylthiopropyl glucosinolate S-oxygenase activity	1.50E-05
GO:0080103	4-methylthiopropyl glucosinolate S-oxygenase activity	1.50E-05
GO:0080104	5-methylthiopropyl glucosinolate S-oxygenase activity	1.50E-05
GO:0080105	6-methylthiopropyl glucosinolate S-oxygenase activity	1.50E-05
GO:0080106	7-methylthiopropyl glucosinolate S-oxygenase activity	1.50E-05
GO:0080107	8-methylthiopropyl glucosinolate S-oxygenase activity	1.50E-05
GO:0018858	benzoate-CoA ligase activity	3.90E-05
GO:0047760	butyrate-CoA ligase activity	3.90E-05
GO:0033946	xyloglucan-specific endo-beta-1,4-glucanase activity	4.20E-05
GO:0030246	carbohydrate binding	7.50E-05

Table S2. (Cont'd.).

GO.ID	Term	*Q* - value
	WT-CT VS WT-SS	
GO:0033506	glucosinolate biosynthetic process from homomethionine	2.60E-07
GO:0010583	response to cyclopentenone	8.50E-07
GO:0000966	RNA 5'-end processing	9.60E-07
GO:0006270	DNA replication initiation	1.80E-06
GO:0051238	sequestering of metal ion	3.50E-06
GO:0016068	type I hypersensitivity	5.00E-06
GO:0080167	response to karrikin	5.40E-06
GO:0051225	spindle assembly	1.30E-05
GO:0009611	response to wounding	1.70E-05
GO:0016572	histone phosphorylation	1.80E-05
GO:0006949	syncytium formation	2.10E-05
GO:0019344	cysteine biosynthetic process	2.60E-05
GO:0010389	regulation of G2/M transition of mitotic cell cycle	3.20E-05
GO:0009734	auxin-activated signaling pathway	3.40E-05
GO:0006749	glutathione metabolic process	4.00E-05
GO:2000026	regulation of multicellular organismal development	7.40E-05
GO:0036065	fucosylation	0.0001
GO:0009694	jasmonic acid metabolic process	0.00012
GO:0048438	floral whorl development	0.0002
GO:0042938	dipeptide transport	0.00023
GO:0018874	benzoate metabolic process	0.00029
GO:0015691	cadmium ion transport	0.00034
GO:0015824	proline transport	0.00036
GO:0060416	response to growth hormone	0.00038
GO:0009828	plant-type cell wall loosening	0.00039
GO:0080148	negative regulation of response to water deprivation	0.00042
GO:0048645	organ formation	0.00047
GO:0042547	cell wall modification involved in multidimensional cell growth	0.00048
GO:0010043	response to zinc ion	0.00049
GO:0019605	butyrate metabolic process	0.00049
GO:0048437	floral organ development	0.00049
GO:0010951	negative regulation of endopeptidase activity	0.0005
GO:0042555	MCM complex	2.10E-06
GO:0048046	apoplast	1.10E-05
GO:0009505	plant-type cell wall	1.30E-05
GO:0000786	nucleosome	0.00033
GO:0004016	adenylate cyclase activity	2.10E-07
GO:0080102	3-methylthiopropyl glucosinolate S-oxygenase activity	2.60E-07
GO:0080103	4-methylthiopropyl glucosinolate S-oxygenase activity	2.60E-07
GO:0080104	5-methylthiopropyl glucosinolate S-oxygenase activity	2.60E-07
GO:0080105	6-methylthiopropyl glucosinolate S-oxygenase activity	2.60E-07
GO:0080106	7-methylthiopropyl glucosinolate S-oxygenase activity	2.60E-07
GO:0080107	8-methylthiopropyl glucosinolate S-oxygenase activity	2.60E-07
GO:0004499	N,N-dimethylaniline monooxygenase activity	7.80E-07
GO:0043295	glutathione binding	1.20E-06
GO:0004364	glutathione transferase activity	2.80E-06
GO:0005507	copper ion binding	9.90E-05
GO:0050661	NADP binding	0.00011
GO:0080046	quercetin 4'-O-glucosyltransferase activity	0.00012
GO:0008107	galactoside 2-alpha-L-fucosyltransferase activity	0.00012
GO:0031625	ubiquitin protein ligase binding	0.00018
GO:0009815	1-aminocyclopropane-1-carboxylate oxidase activity	0.0002
GO:0042936	dipeptide transporter activity	0.00022
GO:0042937	tripeptide transporter activity	0.00022
GO:0050660	flavin adenine dinucleotide binding	0.00029
GO:0004383	guanylate cyclase activity	0.00034
GO:0015334	high-affinity oligopeptide transporter activity	0.00046
GO:0045430	chalcone isomerase activity	0.00049
GO:0018858	benzoate-CoA ligase activity	0.00049
GO:0047760	butyrate-CoA ligase activity	0.00049

Table S2. (Cont'd.).

GO.ID	Term	*Q* - value
	CP-CT VS CP-SS	
GO:0006270	DNA replication initiation	1.90E-25
GO:0008283	cell proliferation	2.10E-25
GO:0051567	histone H3-K9 methylation	2.60E-24
GO:0006275	regulation of DNA replication	3.30E-24
GO:0001510	RNA methylation	9.50E-22
GO:0010389	regulation of G2/M transition of mitotic cell cycle	7.40E-21
GO:0006306	DNA methylation	5.20E-15
GO:0000911	cytokinesis by cell plate formation	1.40E-14
GO:0048453	sepal formation	9.90E-13
GO:0048451	petal formation	4.00E-12
GO:0051225	spindle assembly	3.20E-11
GO:0016572	histone phosphorylation	8.10E-10
GO:0006412	translation	4.90E-08
GO:0080167	response to karrikin	3.40E-07
GO:0006346	methylation-dependent chromatin silencing	4.00E-07
GO:0007018	microtubule-based movement	4.30E-07
GO:0033506	glucosinolate biosynthetic process from homomethionine	1.20E-06
GO:0035720	intraciliary anterograde transport	1.20E-06
GO:0009909	regulation of flower development	1.30E-06
GO:0051238	sequestering of metal ion	1.40E-06
GO:0006084	acetyl-CoA metabolic process	1.90E-06
GO:0000966	RNA 5'-end processing	3.50E-06
GO:0010075	regulation of meristem growth	3.90E-06
GO:0031048	chromatin silencing by small RNA	4.90E-06
GO:0044458	motile cilium assembly	1.20E-05
GO:0080175	phragmoplast microtubule organization	1.30E-05
GO:0006342	chromatin silencing	1.30E-05
GO:0000914	phragmoplast assembly	1.40E-05
GO:0006334	nucleosome assembly	1.50E-05
GO:0006261	DNA-dependent DNA replication	1.60E-05
GO:0016126	sterol biosynthetic process	1.80E-05
GO:0022627	cytosolic small ribosomal subunit	2.90E-17
GO:0005730	nucleolus	2.50E-16
GO:0009506	plasmodesma	4.60E-13
GO:0005618	cell wall	9.20E-10
GO:0009505	plant-type cell wall	6.50E-09
GO:0005794	Golgi apparatus	7.00E-09
GO:0005871	kinesin complex	1.00E-08
GO:0005886	plasma membrane	1.20E-08
GO:0005874	microtubule	6.50E-08
GO:0005774	vacuolar membrane	7.10E-07
GO:0097014	ciliary cytoplasm	7.10E-07
GO:0000786	nucleosome	3.00E-06
GO:0042555	MCM complex	3.60E-06
GO:0048046	apoplast	1.00E-05
GO:0009705	plant-type vacuole membrane	2.00E-05
GO:0003735	structural constituent of ribosome	5.00E-26
GO:0008017	microtubule binding	5.20E-07
GO:0080102	3-methylthiopropyl glucosinolate S-oxygenase activity	1.30E-06
GO:0080103	4-methylthiopropyl glucosinolate S-oxygenase activity	1.30E-06
GO:0080104	5-methylthiopropyl glucosinolate S-oxygenase activity	1.30E-06
GO:0080105	6-methylthiopropyl glucosinolate S-oxygenase activity	1.30E-06
GO:0080106	7-methylthiopropyl glucosinolate S-oxygenase activity	1.30E-06
GO:0080107	8-methylthiopropyl glucosinolate S-oxygenase activity	1.30E-06
GO:0043295	glutathione binding	1.90E-06
GO:0050661	NADP binding	2.10E-06
GO:0004016	adenylate cyclase activity	2.10E-06
GO:0008574	plus-end-directed microtubule motor activity	2.70E-06
GO:0004364	glutathione transferase activity	6.00E-06
GO:0004499	N,N-dimethylaniline monooxygenase activity	6.20E-06

Table S2. (Cont'd.).

GO.ID	Term	*Q* - value
	WT-SS VS CP-SS	
GO:0000966	RNA 5'-end processing	1.60E-07
GO:0033506	glucosinolate biosynthetic process from homomethionine	5.20E-07
GO:0051238	sequestering of metal ion	1.40E-06
GO:0016068	type I hypersensitivity	1.30E-05
GO:0036065	fucosylation	2.70E-05
GO:0006749	glutathione metabolic process	3.20E-05
GO:0010043	response to zinc ion	7.50E-05
GO:0060416	response to growth hormone	0.00011
GO:0006182	cGMP biosynthetic process	0.00026
GO:0015691	cadmium ion transport	0.00028
GO:0016036	cellular response to phosphate starvation	0.00029
GO:0080148	negative regulation of response to water deprivation	0.00057
GO:0042938	dipeptide transport	0.0006
GO:0009611	response to wounding	0.00063
GO:0048544	recognition of pollen	0.00065
GO:0000398	mRNA splicing, via spliceosome	0.00066
GO:0080167	response to karrikin	0.00071
GO:0010951	negative regulation of endopeptidase activity	0.00073
GO:0015850	organic hydroxy compound transport	0.00074
GO:0010231	maintenance of seed dormancy	0.00099
GO:0019605	butyrate metabolic process	0.00114
GO:0009694	jasmonic acid metabolic process	0.00143
GO:0009963	positive regulation of flavonoid biosynthetic process	0.00147
GO:0004016	adenylate cyclase activity	9.60E-09
GO:0043295	glutathione binding	1.30E-08
GO:0004364	glutathione transferase activity	3.20E-08
GO:0080102	3-methylthiopropyl glucosinolate S-oxygenase activity	5.40E-07
GO:0080103	4-methylthiopropyl glucosinolate S-oxygenase activity	5.40E-07
GO:0080104	5-methylthiopropyl glucosinolate S-oxygenase activity	5.40E-07
GO:0080105	6-methylthiopropyl glucosinolate S-oxygenase activity	5.40E-07
GO:0080106	7-methylthiopropyl glucosinolate S-oxygenase activity	5.40E-07
GO:0080107	8-methylthiopropyl glucosinolate S-oxygenase activity	5.40E-07
GO:0004499	N,N-dimethylaniline monooxygenase activity	2.50E-06
GO:0031625	ubiquitin protein ligase binding	3.50E-05
GO:0008107	galactoside 2-alpha-L-fucosyltransferase activity	3.90E-05
GO:0004383	guanylate cyclase activity	5.30E-05
GO:0016717	oxidoreductase activity, acting on paired donors, with oxidation of a pair of donors resulting in the reduction of molecular oxygen to two molecules of water	0.00026
GO:0030247	polysaccharide binding	0.00026
GO:0050661	NADP binding	0.00031
GO:0042561	alpha-amyrin synthase activity	0.00043
GO:0030246	carbohydrate binding	0.00057
GO:0042936	dipeptide transporter activity	0.00064
GO:0042937	tripeptide transporter activity	0.00064
GO:0043531	ADP binding	0.00066
GO:0005507	copper ion binding	0.00067
GO:0010294	abscisic acid glucosyltransferase activity	0.00081
GO:0004713	protein tyrosine kinase activity	0.00086
GO:0030755	quercetin 3-O-methyltransferase activity	0.00091
GO:0030744	luteolin O-methyltransferase activity	0.00091
GO:0033799	myricetin 3'-O-methyltransferase activity	0.00091
GO:0047763	caffeate O-methyltransferase activity	0.00091
GO:0042800	histone methyltransferase activity (H3-K4 specific)	0.00115
GO:0004462	lactoylglutathione lyase activity	0.00116
GO:0018858	benzoate-CoA ligase activity	0.00118
GO:0047760	butyrate-CoA ligase activity	0.00118
GO:0015334	high-affinity oligopeptide transporter activity	0.0013
GO:0052640	salicylic acid glucosyltransferase (glucoside-forming) activity	0.00145
GO:0052641	benzoic acid glucosyltransferase activity	0.00145
GO:0052639	salicylic acid glucosyltransferase (ester-forming) activity	0.00145

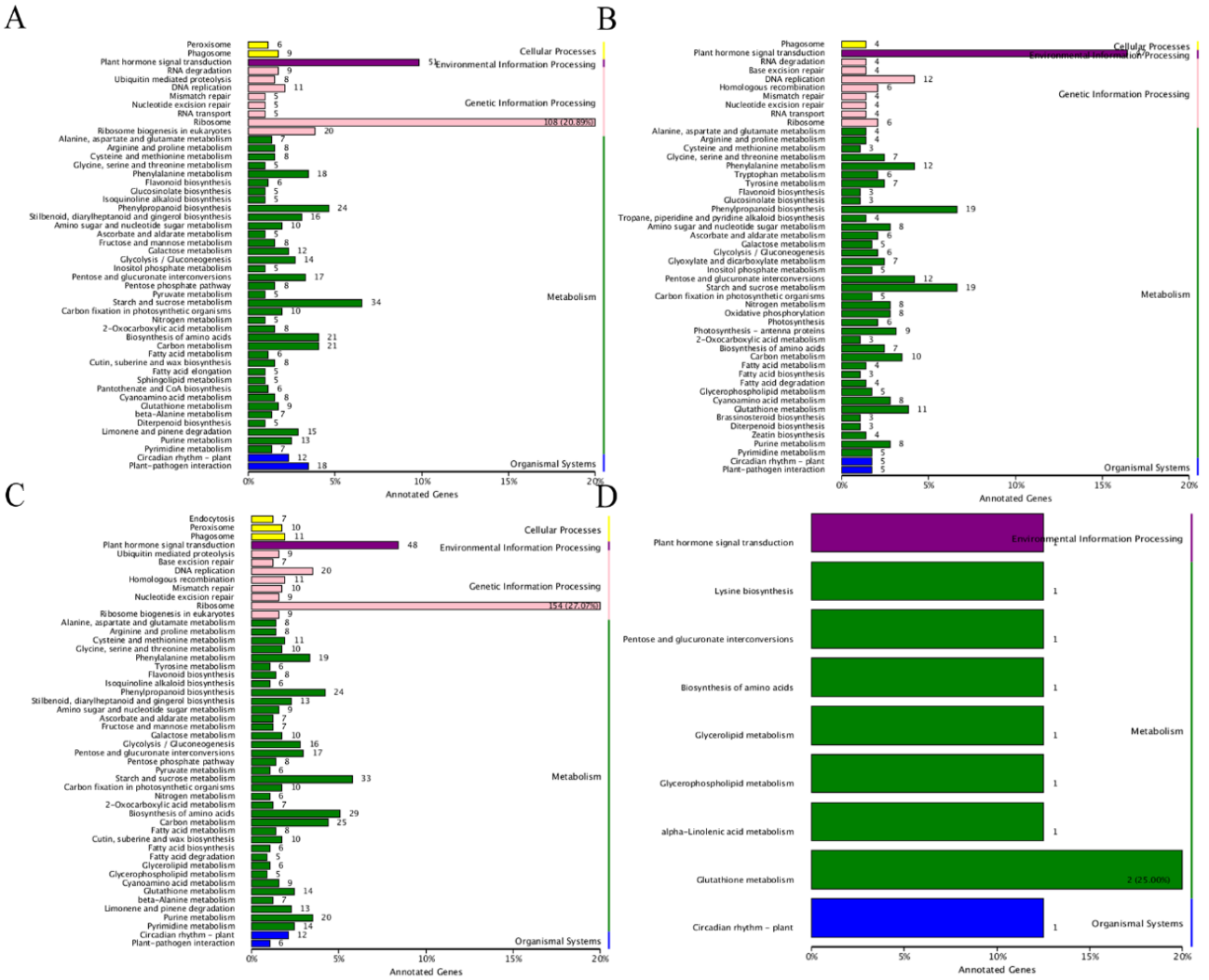

Fig. 4. **KEGG pathways annotation. a** Wild-type control and *SmCP*-transgenic control comparison. **b** Wild-type control and wild type under salt stress comparison. **c** *SmCP*-transgenic lines control and *SmCP*-transgenic lines under salt stress comparison. d Wild type under salt stress and *SmCP*-transgenic lines under salt stress comparison.

Quantitative real-time PCR validation: The transcript abundance of the two genotypes (WT and transgenic) under salt-stress and non-stress conditions were examined. To this end, qRT-PCR analysis was carried out using RNA isolated from *A. thaliana* using the same method as for RNA-seq. Four total RNA extracts with three replications of the two genotypes (WT and transgenic) under the non-stress and salt-stress conditions were used as templates.

The relative expression levels of seven randomly selected genes were dramatically up-regulated and three genes were down-regulated in the CP-CT vs WT-CT comparison (Fig. 6). In addition, six up-regulated genes in the CP-SS vs CP-CT comparison were analyzed. The qRT-PCR results showed consistency with the RNA-seq data, which indicated that the salt resistance mechanism of the experimental materials was reliably revealed by RNA-seq. Thus, we concluded that *SmCP* altered the expression of many salt stress-responsive genes, such as *AT1G56650*, which was down-regulated in the absence of salt-stress treatment, but was up-regulated gene under salt-stress treatment to aid in adaptation to the high-salt environment.

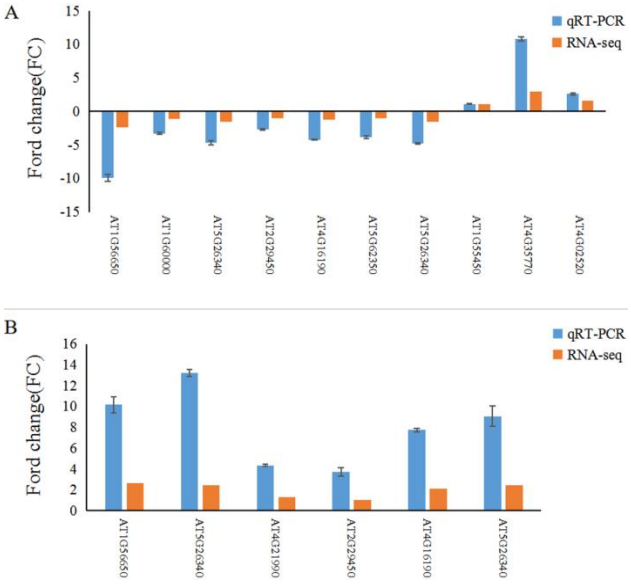

Fig. 6. **Confirmation of RNA-seq expression profiles by qRT-PCR analysis.** Expression ratios presented as fold change in (A) CP-CT/WT-CT. (B) CP-SS/CP-CT. Each experiment included three biological replicates. Values represent the mean ± S.D. CP-CT, *SmCP*-transgenic lines control; WT-CT, wild-type control; CP-SS, *SmCP*-transgenic lines under salt stress.

Table S3. Enrichment KEGG of pathways among DEGs from four comparisons of *SmCP*-transgenic lines and the wild type determined using the top GO software package.

Pathway	KO	Enrichment-Factor	*Q*-value
		WT-CT VS CP-CT	
Ribosome	ko03010	2.75	0
Plant hormone signal transduction	ko04075	1.7	0.006138592
Circadian rhythm - plant	ko04712	2.86	0.044501422
Stilbenoid, diarylheptanoid and gingerol biosynthesis	ko00945	2.23	0.122160533
Ribosome biogenesis in eukaryotes	ko03008	1.95	0.197563147
Starch and sucrose metabolism	ko00500	1.6	0.271150687
Limonene and pinene degradation	ko00903	2.12	0.285094518
Pentose and glucuronate interconversions	ko00040	1.9	0.53019529
Cutin, suberine and wax biosynthesis	ko00073	2.68	0.584136785
Galactose metabolism	ko00052	1.87	1
Flavonoid biosynthesis	ko00941	2.59	1
DNA replication	ko03030	1.91	1
Glucosinolate biosynthesis	ko00966	2.83	1
Diterpenoid biosynthesis	ko00904	2.51	1
Phenylpropanoid biosynthesis	ko00940	1.39	1
Phenylalanine metabolism	ko00360	1.43	1
Pantothenate and CoA biosynthesis	ko00770	1.94	1
Isoquinoline alkaloid biosynthesis	ko00950	1.97	1
Butanoate metabolism	ko00650	2.13	1
beta-Alanine metabolism	ko00410	1.58	1
Sphingolipid metabolism	ko00600	1.68	1
Taurine and hypotaurine metabolism	ko00430	1.94	1
Fructose and mannose metabolism	ko00051	1.39	1
Carbon fixation in photosynthetic organisms	ko00710	1.31	1
Pentose phosphate pathway	ko00030	1.34	1
Valine, leucine and isoleucine biosynthesis	ko00290	1.57	1
Fatty acid elongation	ko00062	1.41	1
alpha-Linolenic acid metabolism	ko00592	1.37	1
Alanine, aspartate and glutamate metabolism	ko00250	1.27	1
Glycolysis / Gluconeogenesis	ko00010	1.13	1
Cyanoamino acid metabolism	ko00460	1.19	1
Carotenoid biosynthesis	ko00906	1.25	1
Ascorbate and aldarate metabolism	ko00053	1.1	1
Tyrosine metabolism	ko00350	1.1	1
Mismatch repair	ko03430	1.1	1
Nitrogen metabolism	ko00910	1.05	1
Steroid biosynthesis	ko00100	1.06	1
ABC transporters	ko02010	1.09	1
2-Oxocarboxylic acid metabolism	ko01210	0.99	1
Plant-pathogen interaction	ko04626	0.98	1
Arginine and proline metabolism	ko00330	0.97	1
Tropane, piperidine and pyridine alkaloid biosynthesis	ko00960	0.95	1
Phagosome	ko04145	0.95	1
Other glycan degradation	ko00511	0.95	1
Glutathione metabolism	ko00480	0.88	1
Base excision repair	ko03410	0.84	1
Folate biosynthesis	ko00790	0.82	1
Zeatin biosynthesis	ko00908	0.82	1
Propanoate metabolism	ko00640	0.79	1
Valine, leucine and isoleucine degradation	ko00280	0.8	1

Table S3. (Cont'd.).

Pathway	KO	Enrichment-Factor	*Q*-value
Porphyrin and chlorophyll metabolism	ko00860	0.79	1
Biosynthesis of unsaturated fatty acids	ko01040	0.73	1
SNARE interactions in vesicular transport	ko04130	0.74	1
Regulation of autophagy	ko04140	0.65	1
Sulfur metabolism	ko00920	0.66	1
Fatty acid metabolism	ko01212	0.72	1
Inositol phosphate metabolism	ko00562	0.7	1
Cysteine and methionine metabolism	ko00270	0.73	1
RNA degradation	ko03018	0.73	1
Amino sugar and nucleotide sugar metabolism	ko00520	0.74	1
Tryptophan metabolism	ko00380	0.6	1
Glycine, serine and threonine metabolism	ko00260	0.66	1
Homologous recombination	ko03440	0.62	1
Peroxisome	ko04146	0.66	1
Purine metabolism	ko00230	0.74	1
Nucleotide excision repair	ko03420	0.64	1
Carbon metabolism	ko01200	0.78	1
Glyoxylate and dicarboxylate metabolism	ko00630	0.57	1
Glycerolipid metabolism	ko00561	0.52	1
Biosynthesis of amino acids	ko01230	0.75	1
Fatty acid biosynthesis	ko00061	0.43	1
Pyruvate metabolism	ko00620	0.54	1
Terpenoid backbone biosynthesis	ko00900	0.46	1
Pyrimidine metabolism	ko00240	0.54	1
Phosphatidylinositol signaling system	ko04070	0.41	1
Glycerophospholipid metabolism	ko00564	0.43	1
Phenylalanine, tyrosine and tryptophan biosynthesis	ko00400	0.32	1
Ubiquitin mediated proteolysis	ko04120	0.48	1
Photosynthesis	ko00195	0.25	1
Endocytosis	ko04144	0.31	1
RNA transport	ko03013	0.26	1
Spliceosome	ko03040	0.19	1
Oxidative phosphorylation	ko00190	0.11	1
Protein processing in endoplasmic reticulum	ko04141	0.12	1
	WT-CT VS WT-SS		
Plant hormone signal transduction	ko04075	2.83	1.51E-09
Photosynthesis - antenna proteins	ko00196	6.69	0.000191332
DNA replication	ko03030	3.77	0.00362644
Phenylpropanoid biosynthesis	ko00940	1.99	0.206270483
Pentose and glucuronate interconversions	ko00040	2.42	0.25205018
Nitrogen metabolism	ko00910	3.04	0.290333491
Brassinosteroid biosynthesis	ko00905	6.13	0.74435289
Tyrosine metabolism	ko00350	2.79	0.818503634
Starch and sucrose metabolism	ko00500	1.62	1
Glutathione metabolism	ko00480	1.93	1
Cyanoamino acid metabolism	ko00460	2.15	1
Ascorbate and aldarate metabolism	ko00053	2.39	1
Zeatin biosynthesis	ko00908	2.97	1
Phenylalanine metabolism	ko00360	1.72	1
Tryptophan metabolism	ko00380	2.18	1
Glucosinolate biosynthesis	ko00966	3.07	1
Circadian rhythm - plant	ko04712	2.15	1

Table S3. (Cont'd.).

Pathway	KO	Enrichment-Factor	*Q*-value
Diterpenoid biosynthesis	ko00904	2.73	1
Glyoxylate and dicarboxylate metabolism	ko00630	1.79	1
Glycine, serine and threonine metabolism	ko00260	1.66	1
Flavonoid biosynthesis	ko00941	2.34	1
Homologous recombination	ko03440	1.69	1
Sesquiterpenoid and triterpenoid biosynthesis	ko00909	2.04	1
Tropane, piperidine and pyridine alkaloid biosynthesis	ko00960	1.72	1
Fatty acid degradation	ko00071	1.64	1
Mismatch repair	ko03430	1.6	1
Base excision repair	ko03410	1.52	1
Galactose metabolism	ko00052	1.41	1
Photosynthesis	ko00195	1.34	1
Ubiquinone and other terpenoid-quinone biosynthesis	ko00130	1.53	1
Inositol phosphate metabolism	ko00562	1.26	1
Alanine, aspartate and glutamate metabolism	ko00250	1.31	1
Isoquinoline alkaloid biosynthesis	ko00950	1.42	1
Carbon fixation in photosynthetic organisms	ko00710	1.19	1
beta-Alanine metabolism	ko00410	1.23	1
Sulfur metabolism	ko00920	1.2	1
Amino sugar and nucleotide sugar metabolism	ko00520	1.07	1
Lysine degradation	ko00310	1.26	1
Fatty acid biosynthesis	ko00061	1.17	1
Sphingolipid metabolism	ko00600	1.21	1
Valine, leucine and isoleucine degradation	ko00280	1.09	1
Porphyrin and chlorophyll metabolism	ko00860	1.07	1
Glycerophospholipid metabolism	ko00564	0.97	1
Fatty acid elongation	ko00062	1.02	1
alpha-Linolenic acid metabolism	ko00592	0.99	1
Steroid biosynthesis	ko00100	0.96	1
Glycerolipid metabolism	ko00561	0.94	1
Nucleotide excision repair	ko03420	0.92	1
Biosynthesis of unsaturated fatty acids	ko01040	0.88	1
Arginine and proline metabolism	ko00330	0.87	1
Fatty acid metabolism	ko01212	0.87	1
Glycolysis / Gluconeogenesis	ko00010	0.88	1
Terpenoid backbone biosynthesis	ko00900	0.83	1
Purine metabolism	ko00230	0.83	1
Phagosome	ko04145	0.76	1
SNARE interactions in vesicular transport	ko04130	0.67	1
Oxidative phosphorylation	ko00190	0.77	1
2-Oxocarboxylic acid metabolism	ko01210	0.67	1
Pentose phosphate pathway	ko00030	0.61	1
Pyrimidine metabolism	ko00240	0.69	1
Peroxisome	ko04146	0.6	1
Limonene and pinene degradation	ko00903	0.51	1
Stilbenoid, diarylheptanoid and gingerol biosynthesis	ko00945	0.5	1
RNA degradation	ko03018	0.59	1
Phosphatidylinositol signaling system	ko04070	0.5	1
Carbon metabolism	ko01200	0.67	1
Cysteine and methionine metabolism	ko00270	0.5	1
Plant-pathogen interaction	ko04626	0.49	1
RNA transport	ko03013	0.38	1

Table S3. (Cont'd.).

Pathway	KO	Enrichment-Factor	*Q*-value
Endocytosis	ko04144	0.28	1
Biosynthesis of amino acids	ko01230	0.45	1
Ubiquitin mediated proteolysis	ko04120	0.22	1
Protein processing in endoplasmic reticulum	ko04141	0.22	1
Ribosome	ko03010	0.28	1
		CP-CT VS CP-SS	
Ribosome	ko03010	3.57	1.50E-10
DNA replication	ko03030	3.16	9.86E-05
Cutin, suberine and wax biosynthesis	ko00073	3.04	0.075010663
Circadian rhythm - plant	ko04712	2.6	0.118775875
Flavonoid biosynthesis	ko00941	3.13	0.204840845
Plant hormone signal transduction	ko04075	1.45	0.391253161
Pentose and glucuronate interconversions	ko00040	1.73	1
Mismatch repair	ko03430	2.01	1
Starch and sucrose metabolism	ko00500	1.41	1
Limonene and pinene degradation	ko00903	1.67	1
Stilbenoid, diarylheptanoid and gingerol biosynthesis	ko00945	1.64	1
Isoquinoline alkaloid biosynthesis	ko00950	2.14	1
Homologous recombination	ko03440	1.56	1
Phenylalanine metabolism	ko00360	1.37	1
Phenylpropanoid biosynthesis	ko00940	1.26	1
Indole alkaloid biosynthesis	ko00901	2.74	1
Galactose metabolism	ko00052	1.42	1
Diterpenoid biosynthesis	ko00904	1.83	1
Vitamin B6 metabolism	ko00750	1.9	1
beta-Alanine metabolism	ko00410	1.44	1
Ascorbate and aldarate metabolism	ko00053	1.4	1
Sphingolipid metabolism	ko00600	1.52	1
Glutathione metabolism	ko00480	1.24	1
Taurine and hypotaurine metabolism	ko00430	1.76	1
Alanine, aspartate and glutamate metabolism	ko00250	1.32	1
Base excision repair	ko03410	1.34	1
Zeatin biosynthesis	ko00908	1.49	1
Glycolysis / Gluconeogenesis	ko00010	1.17	1
Riboflavin metabolism	ko00740	1.83	1
Lysine biosynthesis	ko00300	1.54	1
Cyanoamino acid metabolism	ko00460	1.21	1
Carbon fixation in photosynthetic organisms	ko00710	1.19	1
Glycine, serine and threonine metabolism	ko00260	1.19	1
Pentose phosphate pathway	ko00030	1.22	1
Arachidonic acid metabolism	ko00590	1.45	1
Tyrosine metabolism	ko00350	1.2	1
Fatty acid biosynthesis	ko00061	1.17	1
Nitrogen metabolism	ko00910	1.15	1
Fructose and mannose metabolism	ko00051	1.11	1
Purine metabolism	ko00230	1.04	1
Phagosome	ko04145	1.05	1
Tropane, piperidine and pyridine alkaloid biosynthesis	ko00960	1.08	1
Nucleotide excision repair	ko03420	1.04	1
Folate biosynthesis	ko00790	1.12	1
Valine, leucine and isoleucine biosynthesis	ko00290	1.07	1
Fatty acid degradation	ko00071	1.03	1

Table S3. (Cont'd.).

Pathway	KO	Enrichment-Factor	*Q*-value
Peroxisome	ko04146	1	1
Biotin metabolism	ko00780	1.1	1
Pyrimidine metabolism	ko00240	0.98	1
Glucosinolate biosynthesis	ko00966	1.03	1
Glycerolipid metabolism	ko00561	0.95	1
Butanoate metabolism	ko00650	0.97	1
Tryptophan metabolism	ko00380	0.91	1
Histidine metabolism	ko00340	0.91	1
Cysteine and methionine metabolism	ko00270	0.91	1
Biosynthesis of amino acids	ko01230	0.93	1
Other glycan degradation	ko00511	0.87	1
Carotenoid biosynthesis	ko00906	0.85	1
Arginine and proline metabolism	ko00330	0.88	1
Fatty acid metabolism	ko01212	0.88	1
One carbon pool by folate	ko00670	0.82	1
Fatty acid elongation	ko00062	0.77	1
Photosynthesis - antenna proteins	ko00196	0.75	1
Steroid biosynthesis	ko00100	0.73	1
2-Oxocarboxylic acid metabolism	ko01210	0.79	1
Ribosome biogenesis in eukaryotes	ko03008	0.8	1
ABC transporters	ko02010	0.66	1
Porphyrin and chlorophyll metabolism	ko00860	0.71	1
Lysine degradation	ko00310	0.63	1
Carbon metabolism	ko01200	0.85	1
Regulation of autophagy	ko04140	0.59	1
Pantothenate and CoA biosynthesis	ko00770	0.59	1
Sulfur metabolism	ko00920	0.6	1
Ubiquinone and other terpenoid-quinone biosynthesis	ko00130	0.51	1
Valine, leucine and isoleucine degradation	ko00280	0.55	1
Biosynthesis of unsaturated fatty acids	ko01040	0.44	1
Pyruvate metabolism	ko00620	0.59	1
Amino sugar and nucleotide sugar metabolism	ko00520	0.61	1
Phenylalanine, tyrosine and tryptophan biosynthesis	ko00400	0.43	1
Glycerophospholipid metabolism	ko00564	0.49	1
SNARE interactions in vesicular transport	ko04130	0.34	1
Glyoxylate and dicarboxylate metabolism	ko00630	0.39	1
Inositol phosphate metabolism	ko00562	0.38	1
Endocytosis	ko04144	0.49	1
Ubiquitin mediated proteolysis	ko04120	0.49	1
Citrate cycle (TCA cycle)	ko00020	0.27	1
RNA degradation	ko03018	0.37	1
Photosynthesis	ko00195	0.23	1
Plant-pathogen interaction	ko04626	0.3	1
mRNA surveillance pathway	ko03015	0.14	1
Oxidative phosphorylation	ko00190	0.19	1
RNA transport	ko03013	0.19	1
Spliceosome	ko03040	0.21	1
Protein processing in endoplasmic reticulum	ko04141	0.19	1
	WT-SS VS CP-SS		
Glutathione metabolism	ko00480	12.58	0.010127455

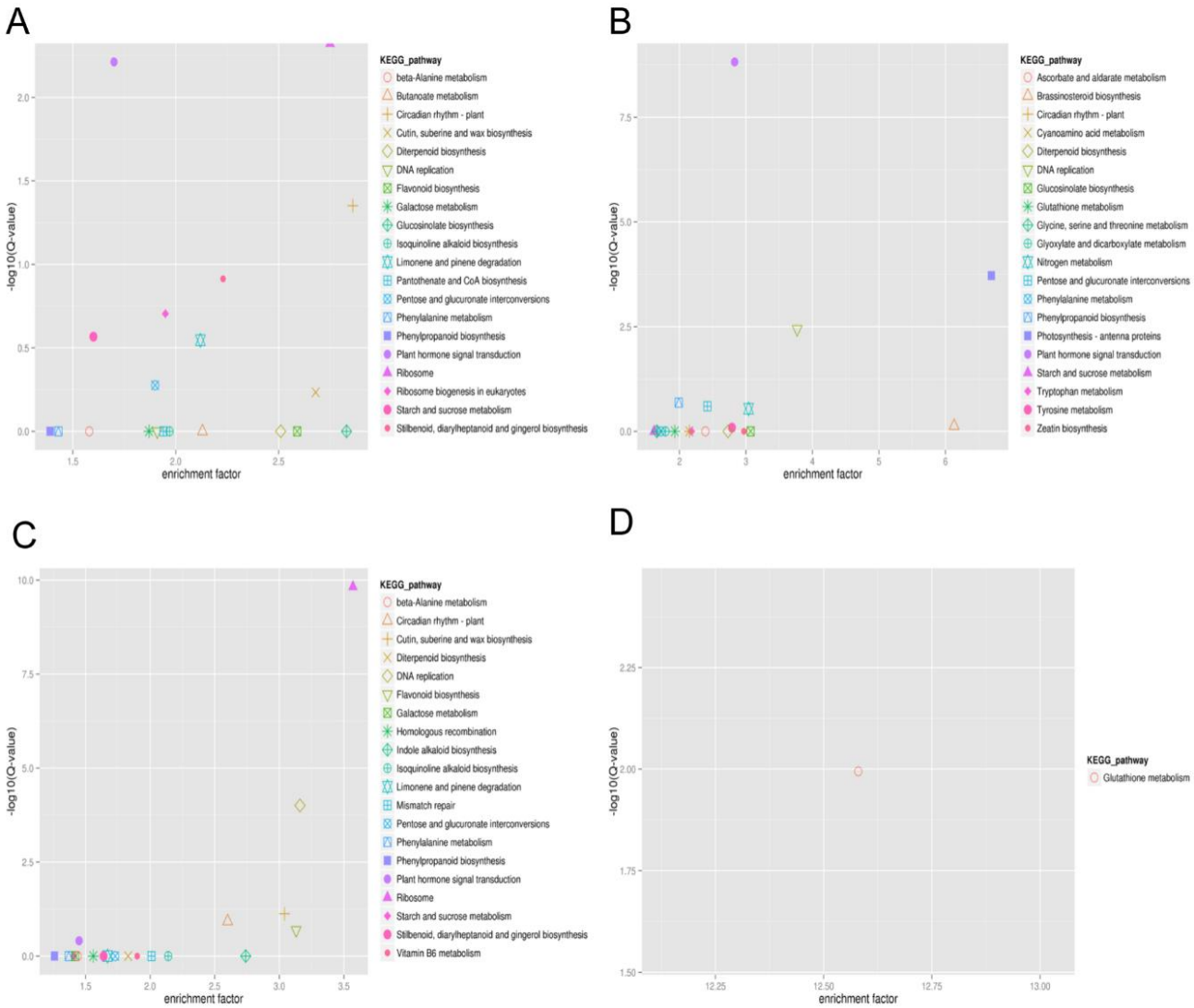

Fig. 5. **KEGG pathway enrichment analysis of DEGs.** The enrichment factor is the ratio of the total number of DEGS to the number of DEGs annotated with the specific pathway. The larger the enrichment factor, the more significant the enrichment level of DEGs with a specific pathway. The ordinate is log10 (*Q* value), where *Q* value is the *P* value after multiple hypothesis testing. Therefore, the larger the ordinate, the more reliable the enrichment of DEGs with the pathway. The closer a point is to the upper right corner, the greater the reference value, and vice versa. The 20 pathways with the most significant concentration (*Q* value minimum) were selected for display.

Discussion

Previous studies have compared differences in the transcriptome of transgenic strains with WT or non-transgenic lines (NT) (Garcia-Molina *et al.*, 2017). Plants must adapt to diverse environmental stresses, including drought, cold, and salinity *etc.*. For example, drought affected the growth of wheat, leading to premature senescence and eventually plant death (Botha *et al.*, 2017). In many cases, transgenes encode proteins that affect simple traits, which are the direct products of protein production. For example, transgenic potato expressing the sweet potato orange gene (*IbOr*) under the control of the stress-inducible *SWAP2* promoter showed significantly increased tolerance to high salinity and oxidative stress mediated by methyl viologen, and increased carotenoids content in the tuber (Cho *et al.*, 2016). The increase in superoxide dismutase (SOD) activity induced by over-expression of the *AhCu/ZnSOD* gene is important in alleviating oxidative damage caused by different environmental stresses (Negi *et al.*, 2015).

However, gene import or deletion is very common, for example, transcription factors affect phenotype expression. *GhWRKY17* increased the drought resistance of transgenic tobacco. Under drought and salt stress, the transcript levels of abscisic acid (ABA) induced genes (*ALEB*, *DRIB*, *NCED*, *EDD*, and *LEA*) were significantly inhibited (Yan *et al.*, 2014). In addition, *GhERF38* is expressed in response to abiotic stresses, such as exogenous ABA treatment and drought (Ma *et al.*, 2017). Similarly, metabolic genes or proteins, such as over-expression of *ZmMKK1*, enhanced expression of ROS-degrading enzymes and ABA-related genes in *A. thaliana* under salt stress and drought, such as peroxidase, catalase, *RAB18* and *RD29A* (Cai *et al.*, 2014). Therefore, stress-resistance genes can affect gene expression in multiple pathways, which includes gene regulation and signal transduction. Thus, a single genetic change can have a substantial physiological or phenotypic impact.

At present, cysteine proteases are still imperfectly known, but previous studies suggest these proteolytic enzymes perform functions in aging and environmental stress. Cysteine proteases participated in nodular development and senescence (van Wyk *et al.*, 2014). In transgenic tobacco plants, the targeted expression of cysteine protease in tapetum cells led to male sterility (Shukla *et al.*, 2016). In parasitic organisms cysteine proteases played crucial roles in tissue penetration, feeding, immunoevasion, virulence, egg hatching, and cycad degeneration (Shareef & Abidi, 2014). It was previously demonstrated that transgenic *Arabidopsis* overexpressing *SmCP* showed enhanced salt tolerance, which may be related to sodium ion excretion and associated changes in the redox state (Zheng *et al.*, 2018). In the present study, we compared the transcriptome changes in *SmCP*-transgenic and untransformed *Arabidopsis* to understand the role of salt stress resistance in molecular function and biological processes. We compared the transcriptome of WT and *SmCP*-over-expression plants under non-stress and salt-stress conditions. Compared with the WT, the scavenging capacity of ROS is enhanced, and the ion efflux ability is enhanced, as a consequence of enhanced salt resistance (Zheng *et al.*, 2018). Accordingly, *GRXS13* (*AT1G03850*) and *NPF5.16* (*AT1G22550*) were up-regulated in response to salt treatment in *SmCP*-over-expression plants compared with the WT. *GRXS13* expression is critical for limitation of basal and photo-oxidative stress-induced ROS (Laporte *et al.*, 2012). *NPF5.16* is a nitrate transporter in *A. thaliana (He et al., 2017)*. These results suggest that *SmCP* over-expression in *A. thaliana* improved salt stress tolerance by influencing redox homeostasis and ion transport.

Acknowledgements

This work was supported by a grant from National Transformation Science and Technology Program (2018ZX08020002-005-003), the National Natural Science Foundation of China (No. 31370600), and the Zhejiang Science and Technology Major Program on Agricultural New Variety Breeding (No. 2016C02056-1).

References

Alzahrani, S.M., I.A. Alaraidh, H. Migdadi, S. Alghamdi, M.A. Khan and P. Ahmad. 2019. Physiological, biochemical, and antioxidant properties of two genotypes of Vicia faba grown under salinity stress. *Pak. J. Bot*, 51(3): 786-798.

Ao, T.G., M.L. Lang, Y.Q. Li, Y. Zhao, L.C. Wang and X.J. Yang. 2016. Cloning and expression analysis of cysteine protease gene (*mwcp*) in *agropyron mongolicum keng*. *Genetics & Mol. Res.,* GMR, 15(1):

Botha, A.M., K.J. Kunert and C.A. Cullis, 2017. Cysteine proteases and *wheat* (*triticum aestivum* L) under drought: A still greatly unexplored association. *Plant, Cell & Environ.*, 40(9): 1679-1690.

Cai, G., G. Wang, L. Wang, Y. Liu, J. Pan and D. Li. 2014. A *maize* mitogen-activated protein kinase kinase, zmmkk1, positively regulated the salt and drought tolerance in transgenic *arabidopsis*. *J. Plant Physiol.*, 171(12): 1003-1016.

Cho, K.S., E.H. Han, S.S. Kwak, J.H. Cho, J.S. Im, S.Y. Hong, H.B. Sohn, Y.H. Kim and S.W. Lee. 2016. Expressing the sweet potato orange gene in transgenic potato improves drought tolerance and marketable tuber production. *Comptes Rendus Biol.*, 339(5-6): 207-213.

Fricke, W., G. Akhiyarova, W. Wei, E. Alexandersson, A. Miller, P.O. Kjellbom, A. Richardson, T. Wojciechowski, L. Schreiber, D. Veselov, G. Kudoyarova and V. Volkov. 2006. The short-term growth response to salt of the developing barley leaf. *J. Exp. Bot.*, 57(5): 1079-1095.

Garcia-Molina, M.D., V. Muccilli, R. Saletti, S. Foti, S. Masci and F. Barro. 2017. Comparative proteomic analysis of two transgenic low-gliadin wheat lines and non-transgenic wheat control. *J. Proteom.*, 165: 102-112.

Han, X., H. Yin, X. Song, Y. Zhang, M. Liu, J. Sang, J. Jiang, J. Li and R. Zhuo. 2016. Integration of small rnas, degradome and transcriptome sequencing in hyperaccumulator *Sedum alfredii* uncovers a complex regulatory network and provides insights into cadmium phytoremediation. *Plant Biotech. J.*, 14(6): 1470-1483.

Hayashi, Y., K. Yamada, T. Shimada, R. Matsushima, N.K. Nishizawa, M. Nishimura and I. Hara-Nishimura. 2001. A proteinase-storing body that prepares for cell death or stresses in the epidermal cells of *arabidopsis*. *Plant & Cell Physiol.*, 42(9): 894-899.

He, Y.N., J.S. Peng, Y. Cai, D.F. Liu, Y. Guan, H.Y. Yi and J.M. Gong. 2017. Tonoplast-localized nitrate uptake transporters involved in vacuolar nitrate efflux and reallocation in *arabidopsis*. *Scientific Reports*, 7(1): 6417.

Huang da, W., B.T. Sherman and R.A. Lempicki. 2009a. Bioinformatics enrichment tools: Paths toward the comprehensive functional analysis of large gene lists. *Nucl. Acids Res.,* 37(1): 1-13.

Huang da, W., B.T. Sherman and R.A. Lempicki. 2009b. Systematic and integrative analysis of large gene lists using david bioinformatics resources. *Nature Protocols*, 4(1): 44-57.

Kim, D., G. Pertea, C. Trapnell, H. Pimentel, R. Kelley and S.L. Salzberg. 2013. Tophat2: Accurate alignment of transcriptomes in the presence of insertions, deletions and gene fusions. *Genom. Biol.*, 14(4): R36.

Koizumi, M., K. Yamaguchi-Shinozaki, H. Tsuji and K. Shinozaki. 1993. Structure and expression of two genes that encode distinct drought-inducible cysteine proteinases in *Arabidopsis thaliana*. *Gene*, 129(2): 175-182.

Laporte, D., E. Olate, P. Salinas, M. Salazar, X. Jordana and L. Holuigue. 2012. Glutaredoxin grxs13 plays a key role in protection against photooxidative stress in *arabidopsis*. *J. Exp. Bot.*, 63(1): 503-515.

Lee, H., C.G. Hur, C.J. Oh, H.B. Kim, S.Y. Pakr and C.S. An. 2004. Analysis of the root nodule-enhanced transcriptome in *soybean*. *Mol. & Cells*, 18(1): 53-62.

Liu, H., W. Wu, K. Hou, J. Chen and Z. Zhao. 2016. Deep sequencing reveals transcriptome re-programming of polygonum multiflorum thunb. Roots to the elicitation with methyl jasmonate. *Mol. Gen. & Genom.,* 291(1): 337-348.

Ma, L., L. Hu, J. Fan, E. Amombo, A.B.M. Khaldun, Y. Zheng and L. Chen. 2017. Cotton gherf38 gene is involved in plant response to salt/drought and aba. *Ecotoxicol.* (*London, England*), 26(6): 841-854.

Minami, A. and H. Fukuda. 1995. Transient and specific expression of a cysteine endopeptidase associated with autolysis during differentiation of *Zinnia mesophyll* cells into tracheary elements. *Plant & Cell Physiol.*, 36(8): 1599-1606.

Mortazavi, A., B.A. Williams, K. McCue, L. Schaeffer and B. Wold. 2008. Mapping and quantifying mammalian transcriptomes by rna-seq. *Nature Methods*, 5(7): 621-628.

Munns, R. 2002. Comparative physiology of salt and water stress. *Plant, Cell & Environ.*, 25(2): 239-250.

Munns, R. and M. Tester. 2008. Mechanisms of salinity tolerance. *Ann. Rev. Plant Biol.*, 59: 651-681.

Negi, N.P., D.C. Shrivastava, V. Sharma and N.B. Sarin. 2015. Overexpression of cuznsod from arachis hypogaea alleviates salinity and drought stress in *tobacco*. *Plant Cell Reports*, 34(7): 1109-1126.

Park, H.J., W.Y. Kim and D.J. Yun. 2016. A new insight of salt stress signaling in plant. *Mol. & Cells*, 39(6): 447-459.

Rahat, Q.U.A., M. Hameed and M.S.A. Ahmad. 2019. Contribution of root structural and functional features towards salinity tolerance in *Diplachne fusca* (L.) P. Beauv. Ex roem. & schult. Subsp. *Fusca*. *Pak. J. Bot.*, 51(3): 773-779.

Shareef, P.A. and S.M. Abidi. 2014. Cysteine protease is a major component in the excretory/secretory products of *Euclinostomum heterostomum* (digenea: Clinostomidae). *Parasitol. Res.*, 113(1): 65-71.

Shukla, P., M. Subhashini, N.K. Singh, I. Ahmed, S. Trishla and P.B. Kirti. 2016. Targeted expression of cystatin restores fertility in cysteine protease induced male sterile *tobacco* plants. *Plant Sci.,* 246: 52-61.

Stanczykiewicz, B., M. Jakubik-Witkowska, A. Polanowski, T. Trziszka and J. Rymaszewska. 2017. An animal model of the procognitive properties of cysteine protease inhibitor and immunomodulatory peptides based on colostrum. *Advances in clinical and experimental medicine* : official organ Wroclaw Medical University, 26(4): 563-569.

Sun, G., Y. Yang, F. Xie, J.F. Wen, J. Wu, I.W. Wilson, Q. Tang, H. Liu and D. Qiu. 2013. Deep sequencing reveals transcriptome re-programming of taxus *x* media cells to the elicitation with methyl jasmonate. *PloS One*, 8(4): e62865.

Tajima, T., A. Yamaguchi, S. Matsushima, M. Satoh, S. Hayasaka, K. Yoshimatsu and Y. Shioi. 2011. Biochemical and molecular characterization of senescence-related cysteine protease-cystatin complex from spinach leaf. *Physiol. Plant.*, 141(2): 97-116.

Trapnell, C., D.G. Hendrickson, M. Sauvageau, L. Goff, J.L. Rinn and L. Pachter. 2013. Differential analysis of gene regulation at transcript resolution with rna-seq. *Nature Biotechnol.*, 31(1): 46-53.

van der Hoorn, R.A. 2008. Plant proteases: From phenotypes to molecular mechanisms. *Ann. Rev. Plant Biol.*, 59: 191-223.

van Wyk, S.G., M. Du Plessis, C.A. Cullis, K.J. Kunert and B.J. Vorster. 2014. Cysteine protease and cystatin expression and activity during *soybean* nodule development and senescence. *BMC Plant Biol.*, 14: 294.

Xu, Y., S. Gao, Y. Yang, M. Huang, L. Cheng, Q. Wei, Z. Fei, J. Gao and B. Hong. 2013. Transcriptome sequencing and whole genome expression profiling of chrysanthemum under dehydration stress. *BMC Genom.,* 14: 662.

Yan, H., H. Jia, X. Chen, L. Hao, H. An and X. Guo. 2014. The cotton wrky transcription factor *ghwrky17* functions in drought and salt stress in transgenic nicotiana benthamiana through aba signaling and the modulation of reactive oxygen species production. *Plant & Cell Physiol.*, 55(12): 2060-2076.

Yang, Y. and Y. Guo. 2018. Elucidating the molecular mechanisms mediating plant salt-stress responses. *The New Phytol.*, 217(2): 523-539.

Ye, Z.H. and J.E. Varner. 1996. Induction of cysteine and serine proteases during xylogenesis in *zinnia elegans*. *Plant Mol. Biol.*, 30(6): 1233-1246.

Zheng, L., S. Chen, L. Xie, Z. Lu, M. Liu, X. Han, G. Qiao, J. Jiang, R. Zhuo and W. Qiu. 2018. Overexpression of cysteine protease gene from *salix matsudana* enhances salt tolerance in transgenic *arabidopsis*. *Environ. & Exp. Bot.*, 147: 53-62.

(Received for publication 4 September 2018)